ARTICLE

A Facile Polyol Route to Uniform Gold Octahedra with Tailorable Size and Their Optical Properties

Cuncheng Li,[†,§] Kevin L. Shuford,[‡] Minghai Chen,[†] Eun Je Lee,[†] and Sung Oh Cho[†,*]

[†]Department of Nuclear and Quantum Engineering, Korea Advanced Institute of Science and Technology, Daejeon, 305-701, Korea, [‡]Chemical Sciences Division, Oak Ridge National Laboratory, Oak Ridge, Tennessee 37-831, and [§]Physical Science and Technology College, Zhengzhou University, Zhengzhou 450052, Henan, P. R. China

ABSTRACT A straightforward and effective polyol route for the controllable synthesis of high-quality gold (Au) octahedra with uniform size is presented in an ethylene glycol solution. Large-scale Au octahedra with the size ranging from tens to hundreds of nanometers were selectively synthesized in high-yield. The surfaces of octahedral Au nanocrystals are smooth and correspond to {111} planes. Formation of Au nanooctahedra was attributed to the preferential adsorption of cationic surfactant poly(diallyldimethylammonium) chloride (PDDA) molecules on the {111} planes of Au nuclei that inhibited the growth rate along the <111> direction. The reduction rate of gold ions in the synthesis process can be rationally manipulated by acidic and basic solutions. This provides a facile and effective route to harvest Au octahedra with different dimensions. The synthetic strategy has the advantage of one-pot and requires no seeds, no foreign metal ions, and no pretreatment of the precursor, so that this is a practical method for controllable synthesis of Au octahedra. Size-dependent optical properties of Au octahedra were numerically and experimentally analyzed. The analysis shows that Au octahedra with sharp edges possess attractive optical properties, promising their applications to surface-enhancement spectroscopy, chemical or biological sensing, and the fabrication of nanodevices.

KEYWORDS: crystal growth · gold · octahedron · polyol synthesis · size tailoring · surface plasmon resonance

Metal nanocrystals have attracted extensive research attention because of their unique properties and various applications to catalysis, biodiagnosis, electronic, photonic, and sensor devices.[1,2] The intrinsic properties of a metal nanocrystal depend strongly on its size and shape.[3,4] Controlled synthesis of metal nanocrystals is thus important for uncovering their properties and for achieving practical applications. Much effort has been devoted to synthesizing various metal nanocrystals with different shapes.[5−21] Among them, metal nanocrystals with sharp edges that dramatically increase electric field enhancement exhibit attractive optical properties,[4,21,22] and thus have promising applications in surface-enhanced spectroscopies, chemical or biological sensing, and the fabrication of nanodevices. This has led to an explosion of interest in synthetic approaches to prepare such metal nanocrystals.

The polyol process[23] is a convenient, versatile, and low-cost route for the preparation of element and alloy metal nanoparticles. In this process, liquid polyol or diol acts both as a solvent of the precursors and as a mild reducing reagent. In recent years, this technique has been further modified through the introduction of shape-controlled polymers, foreign ions, and seeds and combined with careful regulation of reaction temperature for the synthesis of metal nanocrystals with well-defined geometric shapes. A number of regular metal nanocrystals which include truncated tetrahedra,[7] cubes,[6−8,24] bipyramids,[9] octahedra,[8,11,17,25] decahedra,[7,17] icosahedra,[7] one-dimensional (1D) nanowires, nanorods,[26] nanobars,[27,28] and 2D nanoplates[29,30] have been successfully synthesized on the basis of this technique. On the basis of the selective adsorption of surfactant PVP, we reported a polyol synthetic strategy for octahedral Au nanocrystals in a polyethylene glycol 600.[25] Although this approach provided a versatile method of synthesizing Au octahedra, it has a drawback that requires a complex and time-consuming workup procedure for the formation of high-yield Au nanooctahedra. Another polyol route was developed by introducing Ag^+ ions to a 1,5-pentanediol solution. Au colloid synthesized by this method needs a purification process through centrifugation at 500 rpm to remove the big Au particles.[8,31] Moreover, octahedral Au crystals were obtained as the byproduct (<10%) in a polyvinylpyrrolidone (PVP)-mediated polyol process for the synthesis of cubes, truncated tetrahedra, and icosahedra in an ethylene glycol solution.[7]

In addition to polyol synthetic strategies, straight wet-chemical methods were-

*Address correspondence to socho@kaist.ac.kr.

Received for review May 4, 2008 and accepted July 31, 2008.

Published online August 13, 2008.
10.1021/nn800264q CCC: $40.75

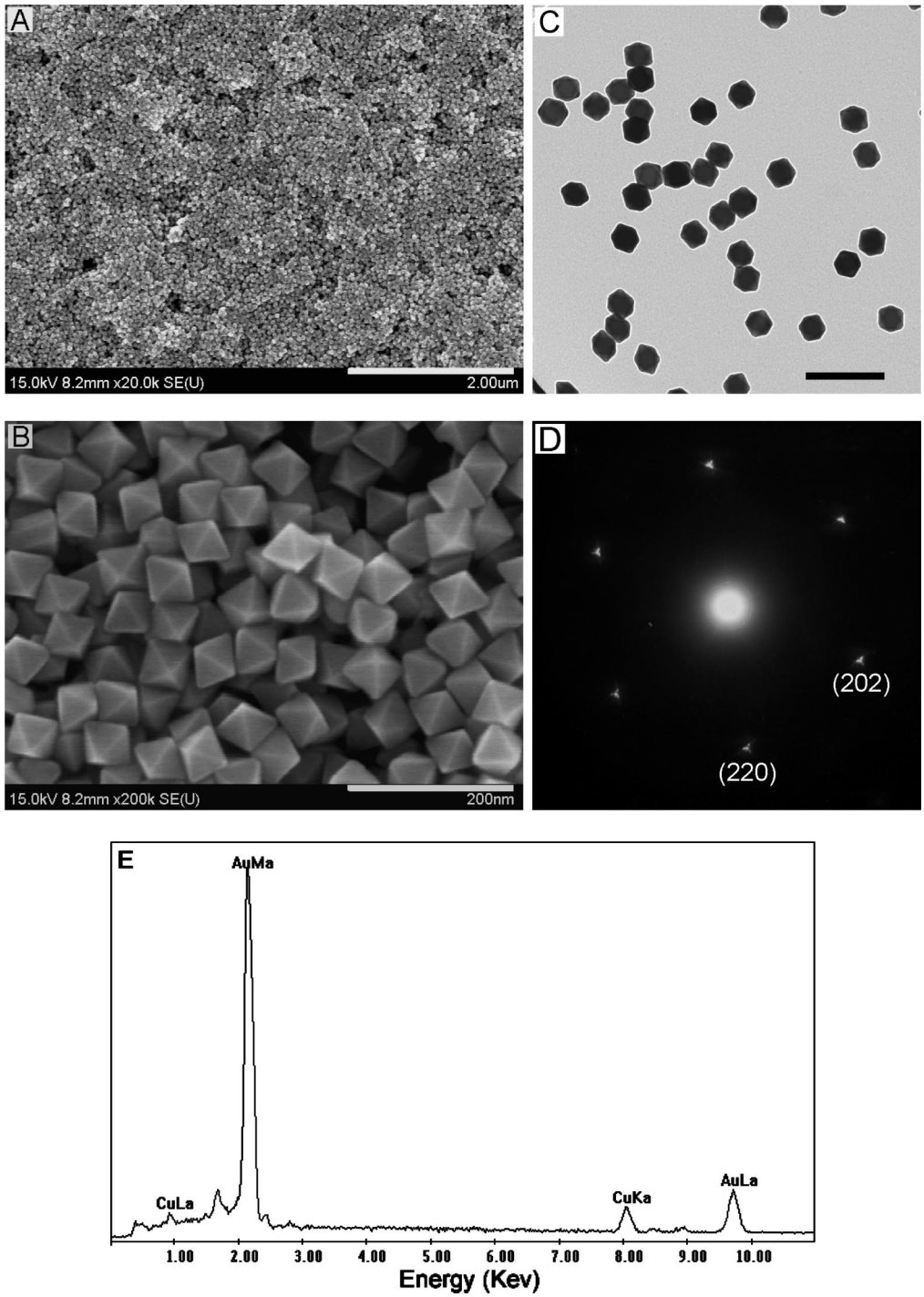

Figure 1. Low magnification (A) and high magnification (B) FESEM images of the as-prepared octahedral Au nanocrystals; TEM image of Au nanooctahedra (C) and SAED pattern (D). The electron beam was perpendicular to one of the triangle faces of an individual octahedral particle. Scale bars for panels A, B, and C are 2 μm, 200 nm, and 200 nm, respectively. Panel E shows the energy dispersive spectrum for the nanooctahedra on the copper grid.

also described by a few groups.[12,32] However, these methods could not afford uniform, high-yield octahedra (yield is about 70∼80%). Alternatively, the seed-mediated preparation pathway employing single-crystal Pt nanoparticles or Au nanorods as seeds for the synthesis of uniform Au octahedra was introduced recently.[33−35] However, to the best of our knowledge, controllable synthesis of single-crystal Pt and Au nanoseeds themselves is also a challenging task. Moreover, it is difficult to directly and systematically tailor the dimension of octahedral Au crystals over a wide range by using the previously reported methods. For example, the maximal size of Au octahedra synthesized by our previous method was limited to <60 nm. The size of Au octahedra generated by chemical sharpening Au nanorods was limited by the length and aspect ratio of Au nanorods.

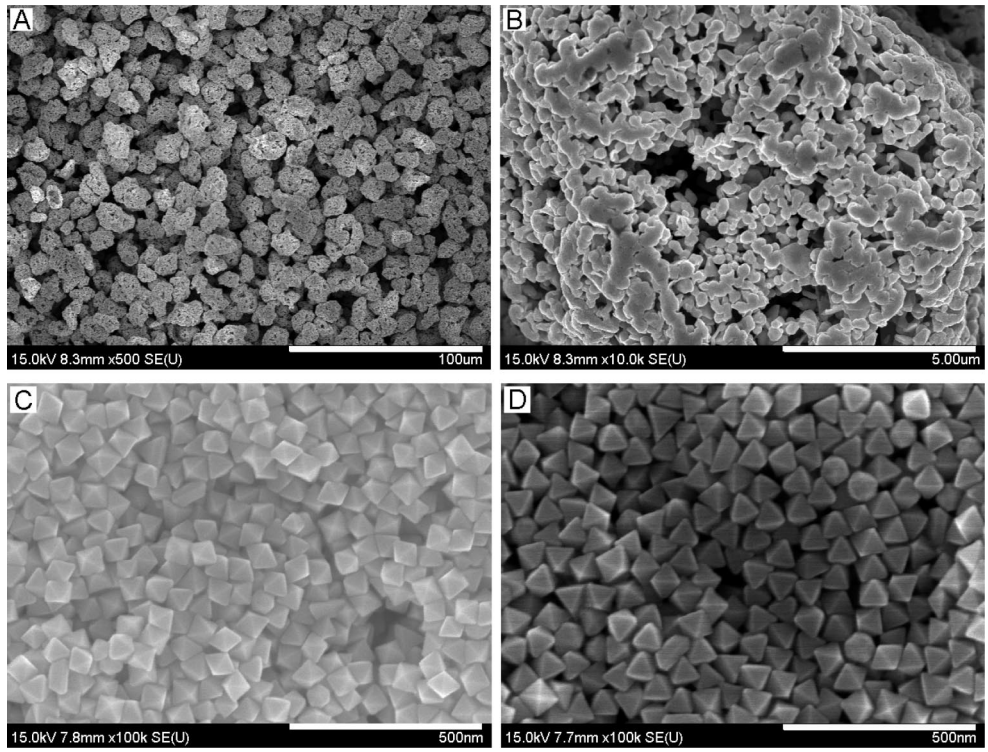

Figure 2. The products synthesized at the reaction temperature of 195 °C in the absence (A,B) and presence (C,D) of surfactant PDDA. The concentrations of PDDA in samples C and D were 5 and 125 mM; the corresponding molar ratios of PDDA to HAuCl4 were 10 and 250, respectively. Scale bars for panels A, B, C, and D are 100 μm, 5 μm, 500 nm, and 500 nm, respectively.

Here, we report a new, facile, and straightforward polyol process for the controllable synthesis of high-quality Au octahedra by using the polyelectrolyte PDDA as stabilizer rather than the traditional PVP. High-yield (>95%, without purification), monodisperse Au octahedra were obtained in a one-pot reaction with a short reaction time of a few tens of minutes. Furthermore, the final size can be readily controlled by introducing acidic and basic solutions into the reaction medium. As a consequence, the dimension of octahedral Au crystals can be straightforwardly and systematically tailored over a wide range. Large-scale, uniform Au octahedra, the size of which ranges from tens to hundreds of nanometers, were selectively and controllably synthesized. Moreover, this synthetic procedure requires no seeds, no foreign metal ions, and no pretreatment of the precursor. The as-prepared octahedral Au nanocrystals were very stable for months due to the electrostatic repulsion and steric stabilization provided by polyelectrolyte PDDA.

For a typical synthesis of Au octahedra, chloroauric acid ($HAuCl_4$) as gold source and PDDA as surfactant were introduced into an ethylene glycol solution in a glass vial. Subsequently, the vial was mounted into an oil bath and heated at 195 °C for 30 min. The final products were collected by centrifugation and washed with water for characterization and property study.

RESULTS AND DISCUSSION

Structural Characterization of Au Nanooctahedra. Field-emission scanning electron microscopy (FESEM, Figure 1A,B) images show that practically all of the products were octahedral nanoparticles. The mean edge length of the octahedral nanoparticles was 50 nm with a standard deviation of 3 nm. All the surfaces of the octahedral nanoparticles were smooth with no obvious defects. The transmission electron microscopy (TEM) image also demonstrates the Au nanoparticles with hexagonal projection were uniform in size (Figure 1C). Figure 1D presents the [001] zone-axis selected area electron diffraction (SAED) pattern recorded by focusing the electron beam on one of the triangle faces of an Au nanooctahedron. The spots with hexagonal symmetry were indexed to {220} reflections, which revealed that each Au nanooctahedron was a single crystal with {111} lattice planes as the basal surfaces. Energy dispersive spectrum (EDS) analysis for such as-prepared sample confirms that the nanooctahedra consist of only gold (see Figure 1E, the copper element came from copper grid).

Influence Factors for the Formation of Au Nanooctahedra. Further experiments revealed that the surfactant PDDA in the solution plays a key role in the synthesis of Au nanooctahedra. When PDDA was absent, $AuCl_4^-$ ions were quickly reduced to Au atoms, which were then agglomerated to form random-shaped Au particles in about 2 min at 195 °C, as typically illustrated

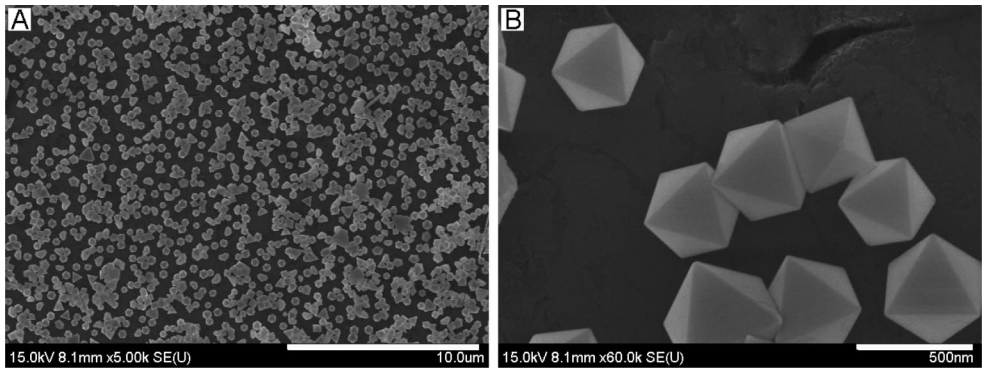

Figure 3. The products synthesized at the reaction temperature of 160 °C with the concentrations of PDDA and $HAuCl_4$ at 25 and 0.5 mM, respectively. Scale bars for panels A and B are 10 μm and 500 nm, respectively.

in Figure 2A,B. This reflects that PDDA is crucial for the formation of octahedral Au nanocrystals. To investigate the effect of the PDDA concentration, a series of experiments were performed without changing other parameters except the PDDA concentration. Interestingly, octahedral Au nanocrystals were produced in high-yield over a wide range of PDDA concentrations from 5 to 125 mM, which corresponds to the molar ratios of PDDA to $HAuCl_4$ of 10 and 250, respectively (Figure 2C,D). This is completely different from the previous reports on the shape evolution of metal nanocrystals using PVP as the surfactant,[29,30] where the crystal shape usually evolved to a sphere at a high molar ratio of PVP to $HAuCl_4$ due to high coverage of PVP on all planes of Au nuclei.

Previous works on the polyol synthesis revealed that an appropriate reaction temperature is essential to obtain the desired product because the reaction temperature greatly affects the reducing power of polyols and the generation rate of source Au atoms.[9,25,29,30] Experiments under different reaction temperatures were thus conducted in this study. Experimental results showed that high-quality Au octahedra were produced dominantly in the temperature ranging from 185 to 195 °C. Moreover, the edge length of Au nanooctahedra was increased from 50 to 60 nm as the reaction temperature was decreased from 195 to 185 °C. This indicates that the low reduction rate of gold ions induced by decreasing the reaction temperature will result in large-sized Au octahedra. When the temperature was further decreased to 160 °C, the product with golden color was deposited on the bottom of the vial after the complete reaction. FESEM images displayed that the products were also dominated by Au octahedra with an edge length of 300∼400 nm, as illustrated in Figure 3. These results indicate that high-yield Au octahedra can be obtained in a wide temperature region and that the size of crystal can be manipulated by changing the reaction temperature. Consequently, the PDDA-mediated polyol process presented here is a reliable and effective synthetic strategy for octahedral Au crystals.

Reduction Process of $AuCl_4^-$ Ions. The essence of the polyol synthesis is the reduction of a metal salt with a polyol or diol in the presence of surfactant. $AuCl_4^-$ ions were generally reduced to Au atoms according to the following reactions.[23,29,30]

$$CH_2OH - CH_2OH \rightarrow CH_3CHO + H_2O \quad (1)$$

$$6CH_3CHO + 2AuCl_4^- \rightarrow 2Au^0 + 3CH_3CO - COCH_3 + 6H^+ + 8Cl^- \quad (2)$$

However, in the present polyol synthesis, the color of the gold precursor changed gradually from yellow to colorless in the initial step (∼6 min). The UV−vis spectrum shows that the absorption band for $AuCl_4^-$ ions disappeared completely, whereas the plasmon band for Au nanocrystals did not appear, indicating no Au nanocrystals were produced. Thus, we believe that the oxidation of gold induced by $AuCl_4^-$ ions also occurred during the reaction process, which resulted in $AuCl_4^-$ ions being evolved to $AuCl_2^-$ ions. That is, the as-formed Au atoms generated by reducing $AuCl_4^-$ ions with aldehyde through reaction 2 were oxidized to $AuCl_2^-$ ions through reactions 3−5. $AuCl_2^-$ ions were finally reduced to Au atoms according to reaction 6. It has been revealed that almost complete evolution of $AuCl_4^-$ ions into $AuCl_2^-$ ions is crucial for the selective formation of octahedral Au nanocrystals.[25]

$$Au^0 + AuCl_4^- + Cl^- \rightarrow AuCl_2^- + AuCl_3^- \quad (3)$$

$$2AuCl_3^- \rightarrow AuCl_2^- + AuCl_4^- \quad (4)$$

$$2Au^0 + AuCl_4^- + 2Cl^- \rightarrow 3AuCl_2^- \quad (5)$$

$$2CH_3CHO + 2AuCl_2^- \rightarrow 2Au^0 + CH_3CO - COCH_3 + 2H^+ + 4Cl^- \quad (6)$$

For the direct proof of the oxidation of Au atoms, an experiment was performed by adding $HAuCl_4$ solution into Au octahedra colloid. In the study, 0.015 mL of 0.5 M $HAuCl_4$ solution was added into 15 mL of 0.5

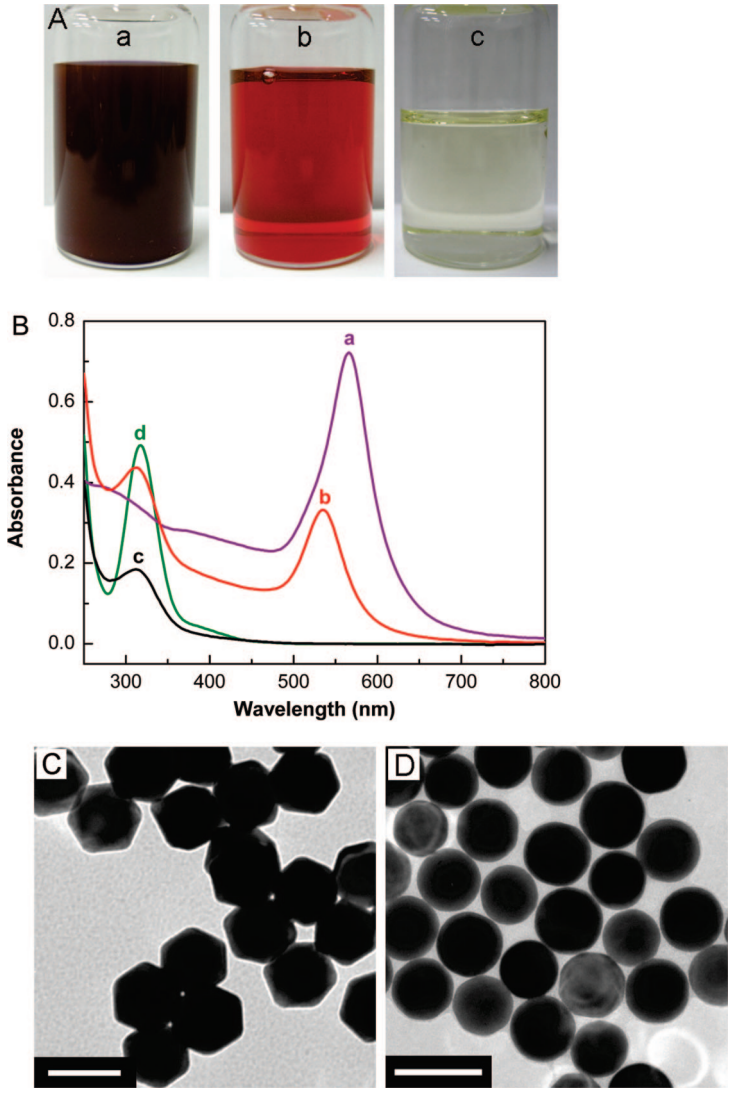

Figure 4. The color change of Au nanooctahedra colloid after introducing a given amount of $HAuCl_4$ solution (A), the corresponding UV−vis spectra (B), and TEM images for sample a and sample b in Figure 4A; scale bar is 50 nm. Photographs in Figure 4A are Au nanooctahedra colloid (a) and Au nanooctahedra colloid together with $HAuCl_4$ solution for 2 min (b) and 2 h (c), respectively. Curves in Figure 4B were recorded when the solution was diluted (×5) with water. Curve d is the absorption spectrum for $HAuCl_4$ solution added to the Au octahedral colloid. The colloid was sampled for optical absorption measurement and TEM observation during the reaction process.

mM, 50 nm Au octahedra colloid (the ratio of Au to $AuCl_4^-$ ions is 1:1); the color of the solution was changed from brown to reddish (2 min), and then to faint yellow (2 h) which is a typical color of $AuCl_4^-$ ions (Figure 4A), indicating that Au octahedra were completely dissolved. The corresponding UV−vis spectra show that the absorption peaks from $AuCl_4^-$ ions and Au nanocrystals decreased synchronously as the reaction time increased (Figure 4B). Moreover, the absorption band of Au crystals was blue-shifted and finally disappeared. This reflects that the size of Au crystals continually decreased, which is consistent with the TEM observation. As shown in Figure 4C,D, the size of Au nanocrystals decreased from 50 to 35 nm when $HAuCl_4$ solution was added into the Au octahedra colloid for 2 min. The shape of Au nanocrystal evolved from octahedron to sphere. The dissolution behaviors of Au octahedra presented here are similar to the previous reports on the dissolution of Au nanoparticles and nanorods induced by $AuCl_4^-$ ions in the presence of cetyltrimethylammonium bromide (CTAB).[36,37]

Formation Mechanism. When the concentration of Au atoms produced by reaction 6 has reached a supersaturation value, they will start to nucleate and grow into Au nanocrystals. As is known, the geometrical shape of a cubical crystal is determined by the ratio (R) of the growth rate along <100> to <111> direction.[38] A perfect octahedral nanocrystal ($R = 1.73$) results from much higher growth rate of the <100> direction than that of the <111> direction. Generally, the selective adsorption of surfactants, ions, ligands, or polymers on a given crystal plane can inhibit the crystalline growth along one specific direction, leading to a preferential growth along another direction.[6−9,11] Therefore, the introduction of an additive with a selective adsorption function is widely used for the synthesis of anisotropic nanocrystals in a solution phase. In our work, surfactant PDDA was introduced as a stabilizer to prevent aggregation of the products. It has been shown that PDDA play an important role in the formation of Au nanooctahedra. PDDA is known to be a cationic polyelectrolyte and thus an initial strong electrostatic interaction between PDDA and $AuCl_4^-$ ions leads to the formation of stable ion pairs. Consequently, the reduction rate of $AuCl_4^-$ ions in the polyol synthesis of Au nanocrystals was decreased in the presence of PDDA. It has been revealed that a slow reaction was favorable for the formation of anisotropic metal nanocrystals.[25,29,30] Under the slow reaction, the growth of metal nuclei can be kinetically controlled through the selective adsorption of polymers or foreign ions introduced in the solution, which leads to final products that deviate from the thermodynamically favored shapes (spheres, cuboctahedra, or multiple twinned particles, etc.). X-ray photoelectron spectra (XPS) and Fourier transform infrared (FTIR) spectroscopy measured for the repeatedly washed sample directly verifies that PDDA molecules were strongly adsorbed on the surface of Au nanooctahedra (not shown here). This suggests that the surfactant PDDA serves not only as a stabilizer to prevent the aggregation of the products but also as a strong shape-controller to assist the formation of octahedral Au crystals through the strong electrostatic interaction with $AuCl_4^-$ ions and through the selective adsorption with Au nuclei during the crystal growth process. On the basis of our results, we can infer that (i) PDDA molecules preferentially adsorb on the {111} planes of Au nuclei, and consequently the growth rate along the <111> direction is reduced while the growth rate along the <100> direction is enhanced, which facilitates the formation of octahedral Au nanocrystals; (ii) an electrostatic repulsion between the surfactant PDDA may in-

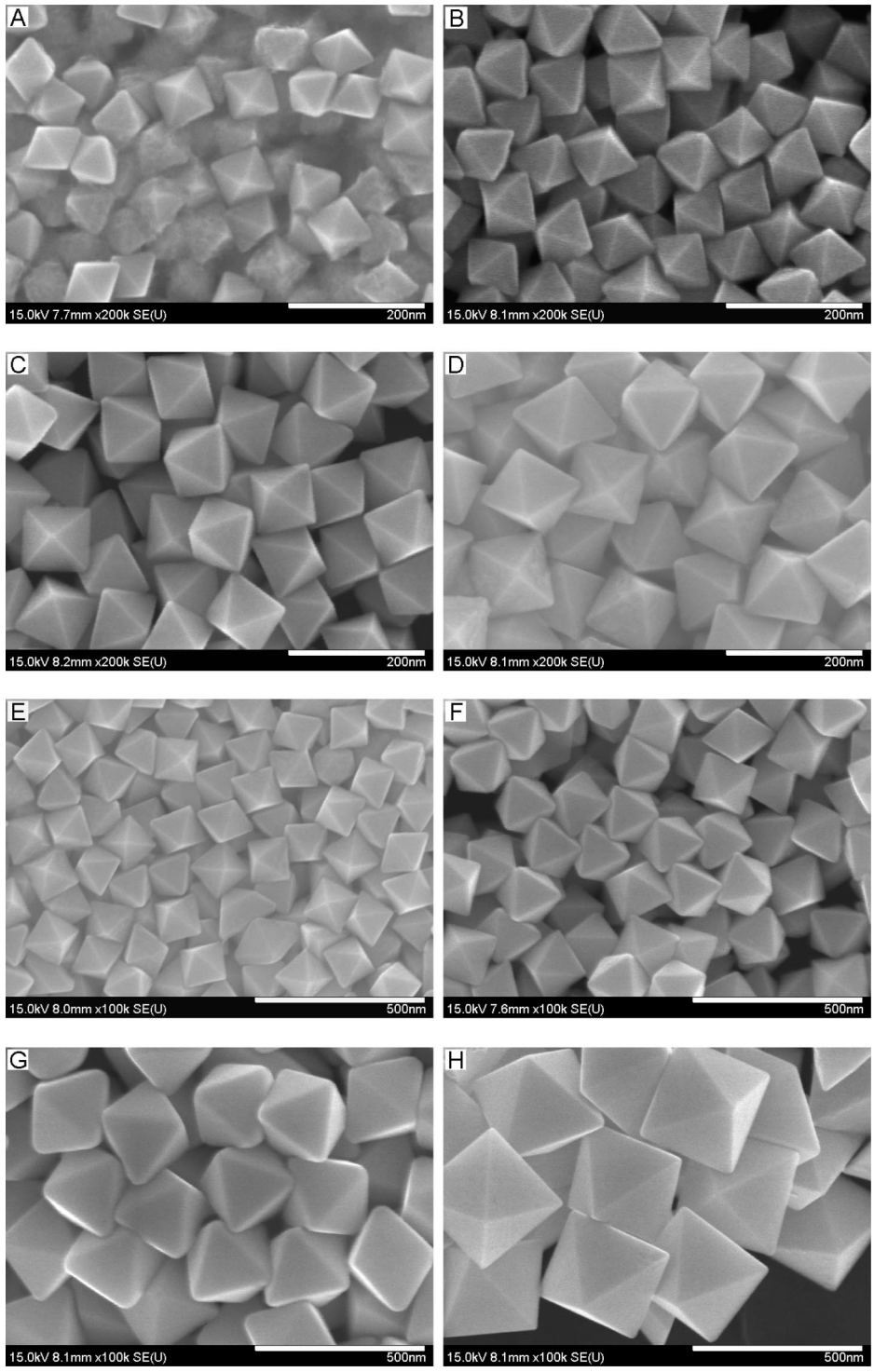

Figure 5. Au octahedra with average edge lengths of 63, 80, 95, 110, 125, 160, 230, and 320 nm (A-H) synthesized at 195 °C by introducing 1 M HCl solution with different amounts (from 0.05 to 0.4 mL) to the initial gold precursor. Scale bars: (A—D) 200 nm, (E—H) 500 nm.

hibit overadsorption on the surfaces of Au crystals, and thus the shape of the major product does not change with the increase of PDDA concentration. Meanwhile, the as-prepared octahedral Au nanocrystals were very stable for months due to the electrostatic repulsion and steric stabilization provided by cationic surfactant PDDA.

Size Tailoring of Au Octahedra. We found that the size of Au octahedra could be further adjusted through introduction of acidic and basic solutions to the initial gold precursor. In this way, Au octahedra with various sizes from tens to hundreds of nanometers were selectively harvested at the reaction temperature of 195 °C. Figure 5 presents the size evolution of Au octahedra along

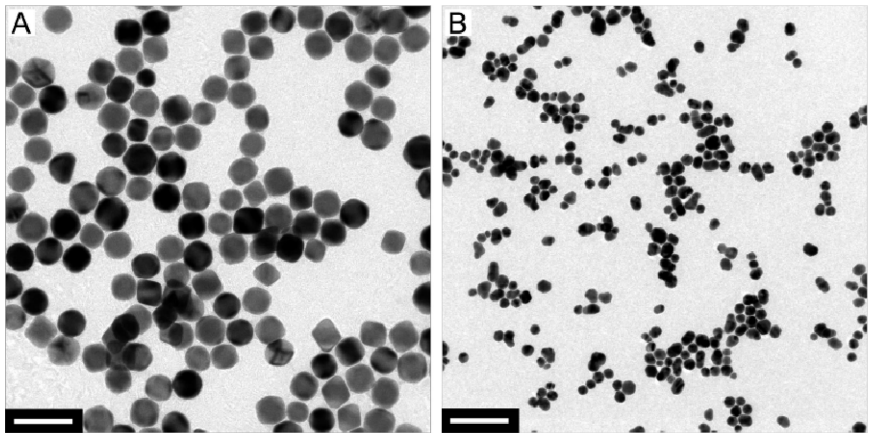

Figure 6. TEM images of Au nanocrystals obtained in the presence of NaOH with different concentration: 1 mM (A) and 3 mM (B). Scale bars are 50 nm.

with the concentration of HCl. Octahedral Au crystals with average edge lengths of 63, 80, 95, 110, 125, 160, 230, and 320 nm were obtained when the concentrations of HCl in the initial gold precursor were 2.5, 5, 7.5, 10, 12.5, 15, 17.5, and 20 mM, respectively. Apparently, the sizes of Au octahedra were increased with the increase of HCl concentration. It was observed in our experiments that the duration of the color change was prolonged and the initial reddish color became faint with increasing HCl concentration. For example, the color of the gold precursor changed to reddish after being heated for about 8 min in the absence of HCl. The light reddish color appeared at about 13 min if the HCl concentration was increased to 20 mM, and finally the products of golden color that is the typical color of big Au crystals were produced. This reflects that HCl can decrease the reduction rate of gold ions, and this provides a new and effective route to synthesize Au crystals with different dimensions by changing the HCl concentration. Moreover, the monodispersity of Au octahedra was less than 10% and the yield of Au octahedra was higher than 90%.

In contrast to the acidic HCl solution, the reduction rate of $AuCl_4^-$ ions could be enhanced by the addition of NaOH solution. We found that a small addition of NaOH expedited the color change of the gold precursor solution and decreased the sizes of the final gold crystals. For example, when 0.02 mL of 1 M NaOH was added into the precursor, a reddish color was observed after 5 min. In this case, the majority of the final products were 20 nm Au nanooctahedra with slightly rounded corners (Figure 6A). In particular, the color of the gold precursor changed immediately from yellow to reddish when the concentration of NaOH reached 3 mM, suggesting the rate of reduction was greatly enhanced. Irregular Au nanoparticles less than 15 nm were produced as the major product (Figure 6B), which further verified that the relatively slow reaction was important for synthesis of metal nanocrystals with well-defined geometric shapes.

The above results suggest that acids and bases can kinetically manipulate the reduction rate of gold ions, and this in turn affects the initial gold nucleation process, which is one of determining factors for the shape and size of the final products. As described above, the oxidation of Au atoms occurred in this study. The oxidation rate of Au atoms was generally increased as the concentration of H^+ ions increased in the reaction medium.[37] Thus, it can be deduced that reduction reaction of gold ions was inhibited to the left if an acidic solution (increase of $[H^+]$ ions in the solution) is added into the initial gold precursor. This causes the generation rate of Au atoms to become slower, and produces bigger Au crystals. On the contrary, when the reduction reaction was driven to the left through the introduction of a basic solution, hydrogen ions are consumed by hydroxyl ions and hence smaller Au crystals are produced.

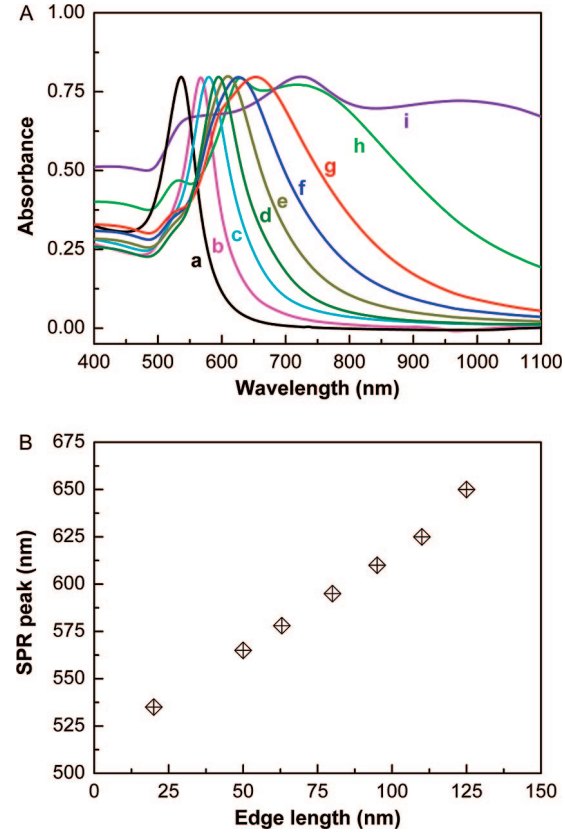

Figure 7. UV−vis absorption spectra for Au octahedra with different edge lengths dispersed in water (A). The edge lengths of Au octahedra from curve a to curve i were 20, 50, 63, 80, 95, 110, 125, 160, and 230 nm, respectively. The absorption peak as a function of the nanooctahedra edge lengths (20∼110 nm) (B).

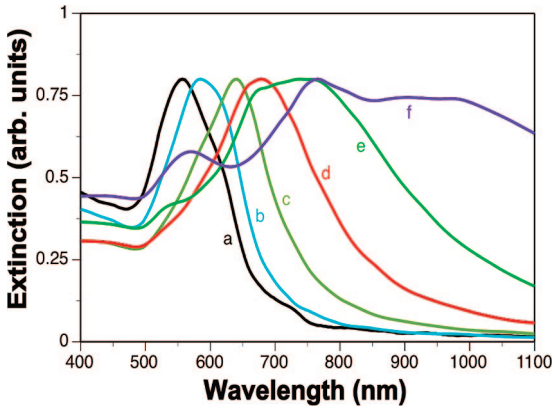

Figure 8. Calculated extinction spectra for Au octahedra with different edge lengths in water. The edge lengths of Au octahedra from curve a to curve f are 20, 63, 95, 125, 160, and 230 nm, respectively.

OPTICAL PROPERTIES

The UV−vis−NIR optical absorption spectra of Au octahedra with different sizes are shown in Figure 7A. Octahedra with edges <110 nm display a single resonance that corresponding to dipole surface plasmon resonances (SPR). The absorption peaks for Au octahedra with edge lengths of 20, 50, 63, 80, 95, and 110 nm were found at 535, 565, 578, 595, 610, and 625 nm, respectively. This shows that the absorption peak position has a linear correlation with the octahedron size (Figure 7B). In addition, the SPR peaks of octahedral Au nanocrystals are red-shifted compared to spherical Au nanoparticles of the same size, which is attributed to the sharp structural features of the octahedra. It has been shown that intense polarizations localized at such features typically induces a red-shift in the absorption spectra.[4] Moreover, as the particles become larger from 20 to 110 nm, the dipole peak broadens and a shoulder at around 540 nm grows. In contrast, large octahedra that have an edge length of 230 nm (trace i in Figure 6A) display three resonances at approximately 565, 760, and 960 nm. The emergence of numerous peaks in the optical spectrum is consistent with multipolar excitation of large metallic nanoparticles.[39−41]

To clarify the origin of the observed resonance peaks of the Au octahedra, we calculated the optical properties of the octahedra in water using the discrete dipole approximation.[42,43] Details regarding the calculation and the method can be found in the Supporting Information (SI). Figure 8 shows the calculated extinction spectra of octahedra with various edge lengths between 20 and 230 nm. The results agree well with experiment and show all of the same trends in the optical spectra observed upon increasing the edge length. The peak widths for particles <100 nm (traces a−c) are slightly wider than those measured experimentally. This is attributed to the apexes of smaller particles being slightly rounded. For small Au octahedra, it has been shown that the sharp tips lead to an interaction between dipole resonances rotated 45° from one another that oscillate parallel to a symmetry plane that bisects the octahedron into square pyramids (designated as in-plane modes). The interaction produces a peak splitting and resonance broadening. This effect is manifested in traces a and c as shoulders found at 625 and 575 nm, respectively. The splitting is also present in trace b, but the intensities are approximately equal leading to a more symmetric peak shape. This interaction decreases substantially as the particles get larger than 100 nm, and the in-plane dipole splitting becomes inconspicuous. Note that there are also out of plane (perpendicular to the symmetry plane) dipole modes that contribute to the excitations at similar wavelengths. As the edge length reaches 160 nm (trace e), the peak centered at 750 nm begins to broaden significantly. The emergence of higher-order excitations is evident at approximately 540 and 675 nm. Three peaks are clearly resolved at 565, 760, and 960 nm for the octahedra with 230 nm edges. A detailed analysis of the induced polarizations (presented in the SI) shows that the peaks at 565 and 760 nm primarily correspond to out of plane and in-plane quadrupole excitations, respectively. The peak at 960 nm results from both in-plane and out of plane dipole excitations that occur at approximately the same wavelength.

CONCLUSIONS

A low cost and straightforward PDDA-mediated polyol route for the controllable synthesis of single-crystalline Au octahedra was presented in an ethylene glycol solution. This is a facile and effective method for rapid and large-scale synthesis of uniform Au octahedra. The dimension of Au octahedra could be tailored from 20 to 320 nm by introducing a given amount of acid and basic solution to the initial gold precursor. Structural characterization by FESEM, TEM, and SAED indicated that the surfaces of the Au nanooctahedron are smooth and correspond to {111} planes. The surfactant PDDA was found to be crucial for the synthesis of octahedral Au nanocrystals. Formation of such Au octahedra is attributed to the preferential adsorption of PDDA on the {111} planes of Au nuclei that inhibited the growth rate along the <111> direction. Size-dependent optical properties of Au octahedra were numerically and experimentally analyzed. We believe that octahedral Au nanocrystals with attractive optical properties could have promising applications to surface-enhanced spectroscopies, chemical or biological sensing, and the fabrication of nanodevices.

METHODS

Synthesis of Au Octahedra. The synthetic procedure for Au nanooctahedra is described below. A 0.4 mL portion of PDDA (M_w = 400000∼500000, 20 wt % in H_2O, Aldrich) and a given amount of 1 M HCl solution (from 0 to 0.4 mL) was added to 20 mL of ethylene glycol (Aldrich) solution in a glass vial. The mixture was stirred with a magnetic blender for 1∼2 min at room temperature and ambient conditions. A 0.02 mL portion of 500 mM chloroauric acid ($HAuCl_4$, Aldrich) aqueous solution was introduced under stirring. The final concentration of $AuCl_4^-$ ions and PDDA in the initial gold precursor was about 0.5 mM and 25 mM, respectively (the molar ratio of PDDA to $AuCl_4^-$ ions was 50). The bottle containing the as-prepared gold precursor solution was sealed and subsequently heated at 195 °C, which is close to the boiling point of ethylene glycol, 198 °C, in an oil-bath for 30 min. During the reaction process, the color of the gold precursor changed gradually from yellow to colorless in the initial step (∼6 min). A reddish color appeared after the gold precursor was heated for 8 min, reflecting the formation of Au nanocrystals. The final product was collected by centrifugation at 15 000 rpm and washed repeatedly with pure water for characterization and optical property study. After the centrifugation, the products were deposited on the bottom of the tubes and the supernatant solution became clear and colorless, indicating no Au nanocrystals existed in the solution. Further experiments, in which the amount of the reagents were controlled to be identical to that of the Au nanooctahedra, were also conducted in order to determine the influences of surfactant PDDA and reaction temperature.

Characterization and Optical Property Measurement. The products were characterized by FESEM (Hitachi S4300 and FEI XL30) and TEM (FEI Tecnai F20). The samples for FESEM were prepared by directly depositing the washed products on the stages. The samples for TEM examination were prepared by putting a droplet of the treated solution on copper grids coated with thin carbon film and then evaporating in air at room temperature. XPS and FTIR measurements for Au nanooctahedra that were repeatedly washed with water were performed using a VG ESCA2000 X-ray photoelectron spectrometer with an Mg Kα excitation source and a Fourier transform infrared spectrophotometer (Shimadzu IRPrestige 21), respectively. For optical measurement, the products were dispersed in water and then optical absorption spectra were recorded with a spectrophotometer (Jasco V530) in the wavelength range of 400−1100 nm, using an optical quartz cell with a 10 mm path-length. The optical properties of the octahedra in water were calculated by using the discrete dipole approximation.[42,43]

Acknowledgment. This work was supported by the Korea Science and Engineering Foundation (KOSEF) grant funded by the Korea government (MOST) (No. 2007-00543). K.L.S. was supported by the Wigner Fellowship Program and the Division of Chemical Sciences, Biosciences, and Geosciences, Office of Basic Energy Sciences, U.S. Department of Energy under contract DE-AC05-00OR22725 with Oak Ridge National Laboratory, managed and operated by UT-Battelle, LLC.

Supporting Information Available: Details regarding the calculation and DDA method. This material is available free of charge *via* the Internet at http://pubs.acs.org.

REFERENCES AND NOTES

1. Daniel, M. C.; Astruc, D. Gold Nanoparticles: Assembly, Supramolecular Chemistry, Quantum-Size-Related Properties, and Applications toward Biology, Catalysis, and Nanotechnology. *Chem. Rev.* **2004**, *104*, 293–346.
2. Rosi, N. L.; Mirkin, C. A. Nanostructures in Biodiagnostics. *Chem. Rev.* **2005**, *105*, 1547–1562.
3. Burda, C.; Chen, X. B.; Narayanan, R.; El-Sayed, M. A. Chemistry and Properties of Nanocrystals of Different Shapes. *Chem. Rev.* **2005**, *105*, 1025–1102.
4. Kelly, K. L.; Coronado, E.; Zhao, L. L.; Schatz, G. C. The Optical Properties of Metal Nanoparticles: The Influence of Size, Shape, and Dielectric Environment. *J. Phys. Chem. B* **2003**, *107*, 668–677.
5. Tao, A. R.; Habas, S.; Yang, P. D. Shape Control of Colloidal Metal Nanocrystals. *Small* **2008**, *4*, 310–325.
6. Sun, Y. G.; Xia, Y. N. Shape-Controlled Synthesis of Gold and Silver Nanoparticles. *Science* **2002**, *298*, 2176–2179.
7. Kim, F.; Connor, S.; Song, H.; Kuykendall, T.; Yang, P. D. Platonic Gold Nanocrystals. *Angew. Chem., Int. Ed.* **2004**, *43*, 3673–3677.
8. Seo, D.; Park, J. C.; Song, H. Polyhedral Gold Nanocrystals with O_h Symmetry: From Octahedra to Cubes. *J. Am. Chem. Soc.* **2006**, *128*, 14863–14870.
9. Wiley, B. J.; Xiong, Y. J.; Li, Z. Y.; Yin, Y. D.; Xia, Y. N. Right Bipyramids of Silver: A New Shape Derived from Single Twinned Seeds. *Nano Lett.* **2006**, *6*, 765–768.
10. Yin, Y.; Erdonmez, C.; Aloni, S.; Alivisatos, A. P. Faceting of Nanocrystals during Chemical Transformation: From Solid Silver Spheres to Hollow Gold Octahedra. *J. Am. Chem. Soc.* **2006**, *128*, 12671–22673.
11. Tao, A.; Sinsermsuksakul, P.; Yang, P. D. Polyhedral Silver Nanocrystals with Distinct Scattering Signatures. *Angew. Chem., Int. Ed.* **2006**, *45*, 4597–4601.
12. Zhang, J.; Gao, Y.; Alvarez-Puebla, R. A.; Buriak, J. M.; Fenniri, H. Synthesis and SERS Properties of Nanocrystalline Gold Octahedra Generated from Thermal Decomposition of $HAuCl_4$ in Block Copolymers. *Adv. Mater.* **2006**, *18*, 3233–3237.
13. Sau, T. K.; Murphy, C. J. Room Temperature, High-Yield Synthesis of Multiple Shapes of Gold Nanoparticles in Aqueous Solution. *J. Am. Chem. Soc.* **2004**, *126*, 8648–8649.
14. Kim, F.; Song, J. H.; Yang, P. D. Photochemical Synthesis of Gold Nanorods. *J. Am. Chem. Soc.* **2002**, *124*, 14316–14317.
15. Chen, S. H.; Wang, Z. L.; Ballato, J.; Foulger, S. H.; Carroll, D. L. Monopod, Bipod, Tripod, and Tetrapod Gold Nanocrystals. *J. Am. Chem. Soc.* **2003**, *125*, 16186–16187.
16. Hao, E.; Bailey, R. C.; Schatz, G. C.; Hupp, J. T.; Li, S. Y. Synthesis and Optical Properties of "Branched" Gold Nanocrystals. *Nano. Lett.* **2004**, *4*, 327–330.
17. Sánchez-Iglesias, A.; Pastoriza-Santos, I.; Pérez-Juste, J.; Rori´guez-González, B.; Abajo, F. J. G.; Liz-Marzán, L. M. Synthesis and Optical Properties of Gold Nanodecahedra with Size Control. *Adv. Mater.* **2006**, *18*, 2529–2534.
18. Jin, R. C.; Cao, Y. W.; Mirkin, C. A.; Kelly, K. L.; Schatz, G. C.; Zheng, J. G. Photoinduced Conversion of Silver Nanospheres to Nanoprisms. *Science* **2001**, *294*, 1901–1903.
19. Jin, R. C.; Cao, Y. C.; Hao, E.; Métraux, G. S.; Schatz, G. C.; Mirkin, C. A. Controlling anisotropic nanoparticle growth through plasmon excitation. *Nature* **2003**, *425*, 487–490.
20. Shankar, S. S.; Rai, A.; Ankamwar, B.; Singh, A.; Ahmad, A.; Sastry, M. Biological Synthesis of Triangular Gold Nanoprisms. *Nat. Mater.* **2004**, *3*, 482–488.
21. Kou, X.; Ni, W.; Tsung, C.-K.; Chan, K.; Lin, H.-Q.; Stucky, G. D.; Wang, J. Growth of Gold Bipyramids with Improved Yield and Their Curvature-Directed Oxidation. *Small* **2007**, *3*, 2103–2113.
22. Pastoriza-Santos, I.; Sánchez-Iglesias, A.; Abajo, F. J. G.; Liz-Marzán, L. M. Environmental Optical Sensitivity of Gold Nanodecahedra. *Adv. Funct. Mater.* **2007**, *17*, 1443–1450.
23. Fievet, F.; Lagier, J. P.; Figlarz, M. Preparing Monodisperse Metal Powders in Micrometer and Submicrometer Sizes by the Polyol Process. *MRS Bull.* **1989**, *14*, 29–34.
24. Im, S. H.; Lee, Y. T.; Wiley, B.; Xia, Y. N. Large-Scale Synthesis of Silver Nanocubes: The Role of HCl in Promoting Cube Perfection and Monodispersity. *Angew Chem. Int. Ed.* **2005**, *44*, 2154–2157.
25. Li, C. C.; Shuford, K. L.; Park, Q.-H.; Cai, W. P.; Li, Y.; Lee, E. J.; Cho, S. O. High-Yield Synthesis of Single-Crystalline Gold Nano-octahedra. *Angew. Chem., Int. Ed.* **2007**, *46*, 3264–3268.
26. Sun, Y. G.; Gates, B.; Mayers, B.; Xia, Y. N. Crystalline Silver Nanowires by Soft Solution Processing. *Nano Lett.* **2002**, *2*, 165–168.

27. Wiley, B. J.; Chen, Y.; McLellan, J. M.; Xiong, Y.; Li, Z.-Y.; Ginger, D.; Xia, Y. N. Synthesis and Optical Properties of Silver Nanobars and Nanorice. *Nano Lett.* **2007**, *7*, 1032–1036.
28. Xiong, Y.; Cai, H.; Wiley, B. J.; Wang, J.; Kim, M. J.; Xia, Y. Synthesis and Mechanistic Study of Palladium Nanobars and Nanorods. *J. Am. Chem. Soc.* **2007**, *129*, 3665–3675.
29. Tsuji, M.; Hashimoto, M.; Nishizawa, Y.; Kubobawa, M.; Tsuji, T. Microwave-Assisted Synthesis of Metallic Nanostructures in Solution. *Chem.—Eur. J.* **2005**, *11*, 440–452.
30. Li, C. C.; Cai, W. P.; Cao, B. Q.; Sun, F. Q.; Li, Y.; Kan, C. X.; Zhang, L. D. Mass Synthesis of Large, Single-Crystal Au Nanosheets Based on a Polyol Process. *Adv. Funct. Mater.* **2006**, *16*, 83–90.
31. Seo, D.; Yoo, C. I.; Park, J. C.; Park, S. M.; Song, H. Directed Surface Overgrowth and Morphology Control of Polyhedral Gold Nanocrystals. *Angew. Chem., Int. Ed.* **2008**, *47*, 763–767.
32. Zhang, J.; Liu, H.; Wang, Z.; Ming, N. Shape-Selective Synthesis of Gold Nanoparticles with Controlled Sizes, Shapes, and Plasmon Resonances. *Adv. Funct. Mater.* **2007**, *17*, 3295–3303.
33. Carbó-Argibay, E.; Rodrı´guez-González, B.; Pacifico, J.; Pastoriza-Santos, I.; Pérez-Juste, J.; Liz-Marzán, L. M. Chemical Sharpening of Gold Nanorods: The Rod-to-Octahedron Transition. *Angew. Chem., Int. Ed.* **2007**, *46*, 8983–8987.
34. Xiang, Y.; Wu, X.; Liu, D.; Feng, L.; Zhang, K.; Chu, W.; Zhou, W.; Xie, S. Tuning the Morphology of Gold Nanocrystals by Switching the Growth of {110} Facets from Restriction to Preference. *J. Phys. Chem. C* **2008**, *112*, 3203–3208.
35. Ni, W.; Kou, X.; Yang, Z.; Wang, J. Tailoring Longitudinal Surface Plasmon Wavelengths, Scattering and Absorption Cross Sections of Gold Nanorods. *ACS Nano* **2008**, *2*, 677–686.
36. Rodrı´guez-Fernández, J.; Pérez-Juste, J.; Mulvaney, P.; Liz-Marzán, L. M. Spatially-Directed Oxidation of Gold Nanoparticles by Au(III)-CTAB Complexes. *J. Phys. Chem. B* **2005**, *109*, 14257–14261.
37. Tsung, C.-K.; Kou, X.; Shi, Q.; Zhang, J.; Yeung, M. H.; Wang, J.; Stucky, G. D. Selective Shortening of Single-Crystalline Gold Nanorods by Mild Oxidation. *J. Am. Chem. Soc.* **2006**, *128*, 5353.
38. Wang, Z. L. Transmission Electron Microscopy of Shape-Controlled Nanocrystals and Their Assemblies. *J. Phys. Chem. B* **2000**, *104*, 1153–1175.
39. Millstone, J. E.; Park, S; Shuford, K. L.; Qin, L; Schatz, G. C.; Mirkin, C. A. Observation of a Quadrupole Plasmon Mode for a Colloidal Solution of Gold Nanoprisms. *J. Am. Chem. Soc.* **2005**, *127*, 5312–5313.
40. Payne, E. K.; Shuford, K. L.; Park, S.; Schatz, G. C.; Mirkin, C. A. Multipole Plasmon Resonances in Gold Nanorods. *J. Phys. Chem. B* **2006**, *110*, 2150–2154.
41. Shuford, K. L.; Ratner, M. A.; Schatz, G. C. Multipolar Excitation in Triangular Nanoprisms. *J. Chem. Phys.* **2005**, *123*, 114713.
42. Draine, B. T. Discrete Dipole Approximation. *Astrophys. J.* **1988**, *333*, 848–872.
43. Draine, B. T.; Flatau, P. J. Discrete-Dipole Approximation for Scattering Calculations. *J. Opt. Soc. Am. A* **1994**, *11*, 1491–1499.